Instability: Dynamic Loading Models

9

Todd McKinley

Clinical Manifestations of Instability

Successful orthopedic management of articular injuries, primarily to prevent post-traumatic osteoarthritis (PTOA), is predicated on reestablishing a long-term mechanical environment in the joint that fosters healthy cartilage mechanotransduction. Clinically, it is emphasized that accurate restoration of joint surface congruity is necessary for that purpose [1–4]. However, the long-term effects of residual incongruity on joint outcomes are inconsistent, and there are many reports of cases or series where patients have done surprisingly well in the presence of substantial incongruity [5–8]. For example, while reduction accuracy plays an important role in outcomes in patients sustaining acetabular fractures [3], reduction accuracy has little effect on patients that sustain tibial plateau fractures [6, 8–10]. Clinical evidence linking incongruity to PTOA is inconclusive, in contrast to consistent observations that instability causes PTOA [11–13].

The rationale to study the mechanical and biologic effects of instability on injured joints is supported by clinical observations consistently relating instability to poor outcomes and PTOA. Patients sustaining acetabular fractures have uniformly poor outcomes in joints with residual instability [3]. Likewise, malaligned and unstable tibial plateau fractures fare poorly long term regardless of joint surface congruity [9, 11, 13]. Finally, patients with congruous but unstable ankles (residual mortise malreduction or chronic ankle sprains) have a high rate of PTOA [12, 14].

While clinicians often describe patients as having unstable joints, the definition of joint instability is nebulous. Clinical manifestations of instability are dominated by sudden catching or giving way of an affected joint. Patients will relate that their affected extremity gives out or that the joint feels loose. This typically occurs during walking and changing directions or during a twisting motion. Such changes in position of the joint surfaces can include excessive translational and rotational displacements. Mechanically, this likely translates into articulating surfaces sustaining sudden unphysiologic changes in position and motion resulting in abnormal loading magnitudes and rates of stress transfer; these loads can be significantly higher than seen in typical physiologic function. These alterations in loading result in abnormal contact patterns, with articular surface contact occurring in regions not habitually oriented to sustaining such stresses or even any contact. Repeated unstable loads accumulated over time develop changes in the affected joint that consistently leads to PTOA. In these patients, the original mechanical symptoms that typify instability evolve into more consistent pain

T. McKinley, M.D. (✉)
Department of Orthopedic Surgery, IU Health Methodist Hospital, Indiana University, North Senate Boulevard, Suite 535, Indianapolis, IN 46202, USA
e-mail: tmckinley@iuhealth.org

S.A. Olson and F. Guilak (eds.), *Post-Traumatic Arthritis: Pathogenesis, Diagnosis and Management*,
DOI 10.1007/978-1-4899-7606-2_9, © Springer Science+Business Media New York 2015

that is characteristic of osteoarthritis. Therefore, understanding the macroscopic and microscopic mechanical effects of instability and how these effects are transduced into a degenerative biologic response of an affected joint is important in understanding PTOA.

The majority of tests investigating pathomechanical residual effects of intra-articular fractures on cartilage have focused on static testing of contact stresses as a function of articular surface displacement, as well as congruity-dependent perturbations in articular surface stress transfer [15–17]. Modeling instability is seemingly more difficult. Instability, by definition, cannot be reproduced in a static testing preparation. Recent improvements in analytical and computational techniques have made instability testing more feasible and meaningful. In this chapter, instability testing in cadaveric studies and computational models will be summarized highlighting articular surface and cartilage interstitial stress perturbations sustained in unstable joints. Subsequently, the effects of instability on cartilage biologic response in tissue-level and living organ-level models will be described.

Cartilage Material Properties and Physiology

The mechanical environment encountered by cartilage, in particular on the joint surface, is heterogenous in terms of a wide variety of stress magnitudes, stress rates, and directions of stress that are transmitted between the articulating structures. Articular cartilage transduces the heterogenous surface loading envelope into a relatively homogenous set of hydrostatic stresses and strains within the substance of the tissue and into the subchondral plate. Articular cartilage has highly evolved structure and complex material properties that optimize load transfer across articulating surfaces and through the interstitium of the tissue [18]. Articular cartilage transmits load by deformation of its solid matrix constituents and through hydrostatic pressurization of the interstitial fluid permeating the solid matrix. Cartilage material properties have been intensely studied in experiments ranging from molecular-level investigations to organ-level investigations. Because of its biphasic nature, stresses developed within cartilage are highly time dependent [18, 19]. Stresses and deformation in loaded cartilage are particularly sensitive to stress rates [18, 20]. The rate dependence on stress and deformation within cartilage that has been shown to affect tissue mechanics on a microscopic scale to the level chondrocyte deformation have been shown to be biologically relevant as biosynthetic responses at the chondrocyte level are primarily a function of loading rate. Likewise, tissue-level experiments have shown that biosynthesis of DNA, collagen, and proteoglycans is primarily affected by changes in stress rates [21, 22]. Similarly, mechanical damage of cartilage and biosynthetic response of cartilage to injurious impact loading have both been shown to be primarily load-rate dependent [23–25].

These studies highlight the importance of accurately reproducing physiologic and pathologic loading rates in cartilage investigations. Dynamic testing is especially pertinent in unstable joints because these joints will invariably include regions of cartilage with accentuated high stress rates and stress magnitude peaks. Therefore, simulating realistic stresses and stress rates during in vitro and in vivo preparations takes on increased importance in instability investigations. Recent improvements in real-time stress transducers have facilitated accurate physical testing of unstable and incongruous joints. In addition, computational methods that account for time-dependent cartilage structural and material properties and survey accurate motion encountered in physiologic joint duty cycles have provided new information on cartilage mechanics in normal and unstable conditions.

Macromechanical Tests of Instability

Contact Stress Rate Changes During Instability

Joint instability was simulated in a dynamic model using human cadaveric ankles. In this model, human cadaveric ankles were manipulated

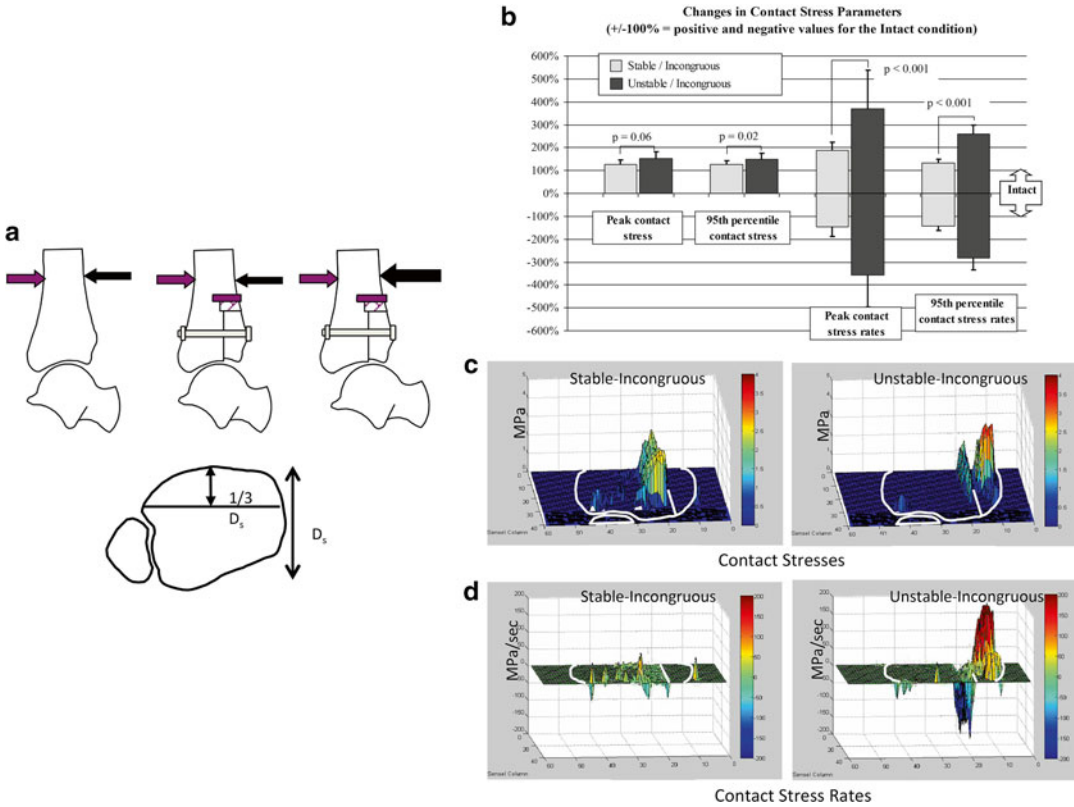

Fig. 9.1 Dynamic human cadaveric ankle loading model in which ankles were made incongruous with a coronally directed osteotomy of the anterior distal tibial surface displaced proximally 2.0 mm (**a**). Anterior and posterior forces were applied to the tibia through pneumatic cylinders to affect the stability of the joint. Incrementally increasing pulses were applied posteriorly to the tibia (**a**, *black arrow*) until subluxation occurred during loading. Changes in contact stress in stable-incongruous and unstable-incongruous specimens were modest compared to intact specimens (**b**). In contrast, contact stress rates increased dramatically in unstable-incongruous specimens compared to stable-incongruous specimens (**b**). Contour maps clearly depict relative equivalence in changes in contact stress peaks (**c**) and significant differences in contact stress rate peaks (**d**) that occurred during instability

to create a "metastable" articulation in which joint subluxation could be reproduced during normal joint motion with minimal changes in external loading conditions [26]. This allowed the investigators to sample contact stresses under incongruous conditions with nearly identical extrinsic loading in ankles that either remained stable or had an obvious instability event. The premise of the study was to simultaneously compare the effects of incongruity and instability on articular surface stress transfer.

In this model, the distal tibial surface was made incongruous by osteotomizing the anterior one-third of the distal tibia. The fragment was proximally displaced 2.0 mm and secured with internal fixation creating a coronally directed stepoff and a defect into which potential subluxation of the talus could occur (Fig. 9.1a). Subsequently, specimens were mounted into a custom fabricated dynamic ankle loading fixture that maintained physiologic motion of the ankle, hindfoot, and midfoot. The loading fixture was secured to a MTS machine that subjected specimens to physiologic loads and motion encountered during the stance phase of walking.

During testing, anteriorly and posteriorly directed forces were applied to the tibia to modulate the sagittal tibiotalar relationship and ultimately the stability of the ankle joint (Fig. 9.1a). Increasing incremental posteriorly directed

pulses were applied to the tibia during the gait cycle until the talus grossly subluxated anteriorly into the distal tibial defect during loading. Stresses were captured at a 132 Hz sampling frequency with a pliable piezoelectric real-time stress transducer that was inserted into the ankle joint. Raw data were used to calculate ankle joint contact stress and contact stress rates throughout the motion cycle.

Contact stresses and contact stress rates were compared under metastable conditions within each specimen. Attention was focused on comparing stress measurements between the last cycle in which the talus remained stable beneath the distal tibia (pre-instability cycle termed stable-incongruous) and the first cycle in which the talus subluxated into the distal tibial defect (instability cycle termed unstable-incongruous). Loading conditions were nearly identical between these two tests with identical motion and axial load, and only a 20 N increase in the posteriorly directed impulse applied to the tibia in the unstable-incongruous trial. Therefore, the effects of incongruity with or without instability could be measured.

Peak contact stresses were only 25 % higher in unstable-incongruous specimens compared to stable-incongruous specimens. In contrast, changes in contact stress rates increased 170 % in unstable-incongruous specimens compared to stable-incongruous specimens (Fig. 9.1b). These data clearly depicted the effects of instability. The rapid rise in contact stresses resulting in the increases in contact stress rates occurred over approximately 5 ms and the entire subluxation event lasted approximately 25 ms which was felt to be physiologically relevant. Real-time contact stress and contact stress rate contour plots demonstrate relative equivalence in peak contact stresses in incongruous ankles regardless of instability (Fig. 9.1c). However, the sharp peak in contact stress rate was clearly evident in unstable ankles (Fig. 9.1d). The instability event studied in this experiment was admittedly idiosyncratic. However, the experiment was designed to create conditions in which the talus would subluxate with minimal additional differences in extrinsic loading between stable and unstable conditions allowing the investigators to focus on the mechanical aberrations that occur primarily due to instability in already incongruous joints.

Contact Stress Directional Gradient Changes During Instability

Using an identical cadaveric ankle incongruity/instability model, the effects of incongruity and instability on contact stress directional gradients were determined under metastable conditions [27]. In this experiment, the researchers used regional contact stress measurements to calculate directional stress magnitude vectors (Fig. 9.2a). Peak transient directional gradients nearly doubled in unstable-incongruous specimens compared to intact specimens and increased 50 % in unstable-incongruous specimens compared to stable-incongruous specimens (Fig. 9.2b). Interestingly, under intact conditions, directional gradients were typically randomly oriented throughout the ankle motion cycle at any specific location and low magnitude (Fig. 9.2c left figure). When these individual vectors were summed over the entire motion cycle, the resultant vectors at each locus in intact ankles were close to zero. The authors concluded that small magnitude randomly oriented directional gradient vectors optimized interstitial stresses to maintain homogenous interstitial fluid distribution and healthy chondrocyte mechanotransduction. In contrast, directional gradients were higher in magnitude and preferentially oriented in incongruous specimens and the magnitudes increased significantly secondary to instability (Fig. 9.2c right two figures). Consistent high-magnitude directional gradients with a consistent orientation would increase shearing deformation of regional chondrocytes which has been shown to result in compromised mechanotransduction and cartilage degeneration. Additionally, this type of oriented stress distribution could lead to regions of interstitial fluid depletion.

In conclusion, human cadaveric testing using an ankle model has been used to develop a physiologically relevant macroscopic model of articular instability. Investigators have created an instability event and quantified resultant changes

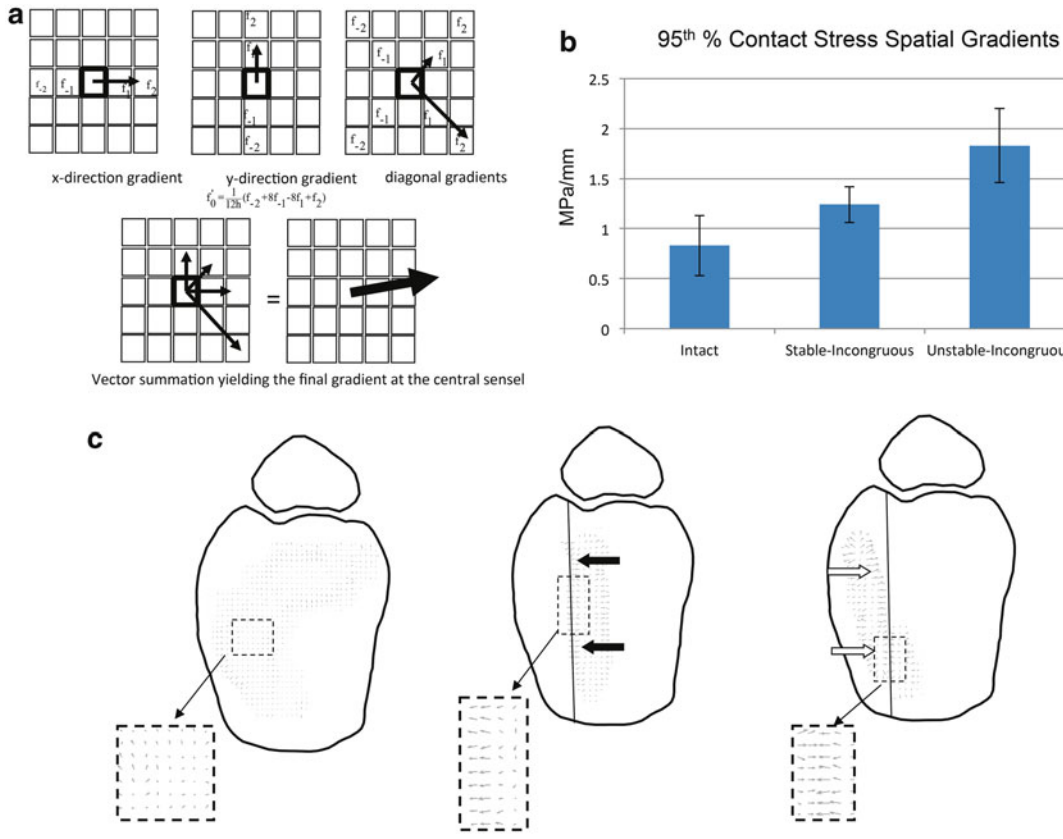

Fig. 9.2 Contact stress directional gradients were calculated by calculating a local derivative at each stress transducer sensel (f_0) based on values of neighboring sensels (**a**). Unstable-incongruous specimens had 100 and 50 % increases in 95th percentile spatial gradient values compared to intact and stable-incongruous conditions (**b**). *Vector plots* demonstrate low-magnitude randomly oriented spatial gradients in intact specimens in contrast to polarized higher magnitude vectors in stable-incongruous and unstable-incongruous specimens (**c**)

in articular surface stress transfer. Significant increases in contact stress rates and contact stress directional gradients were documented in incongruous specimens with instability compared to incongruous specimens that remained stable. Typical contact stress rates during instability under these conditions ranged between 100 MPa/s and 200 MPa/s.

Computational Models of Instability

Cadaveric macromechanical models quantify changes in surface stresses allowing measurements of pressure peaks and calculations of time and directional gradients. However, they do not quantify interstitial cartilage stresses and deformations resulting under both normal conditions and under pathologic conditions such as instability and incongruity. Currently, there are limited analyses that allow direct interstitial stress and strain measurements in loaded cartilage. Therefore, investigators have had to rely on computational methods to simulate such information. However, as outlined above, cartilage material properties are complex highlighting the difficulty and ultimately the importance of sophisticated computational methods to accurately simulate interstitial cartilage deformation and stress fields under load.

Goreham-Voss and colleagues developed a transversely isotropic poroelastic finite element model that could simulate unstable motion

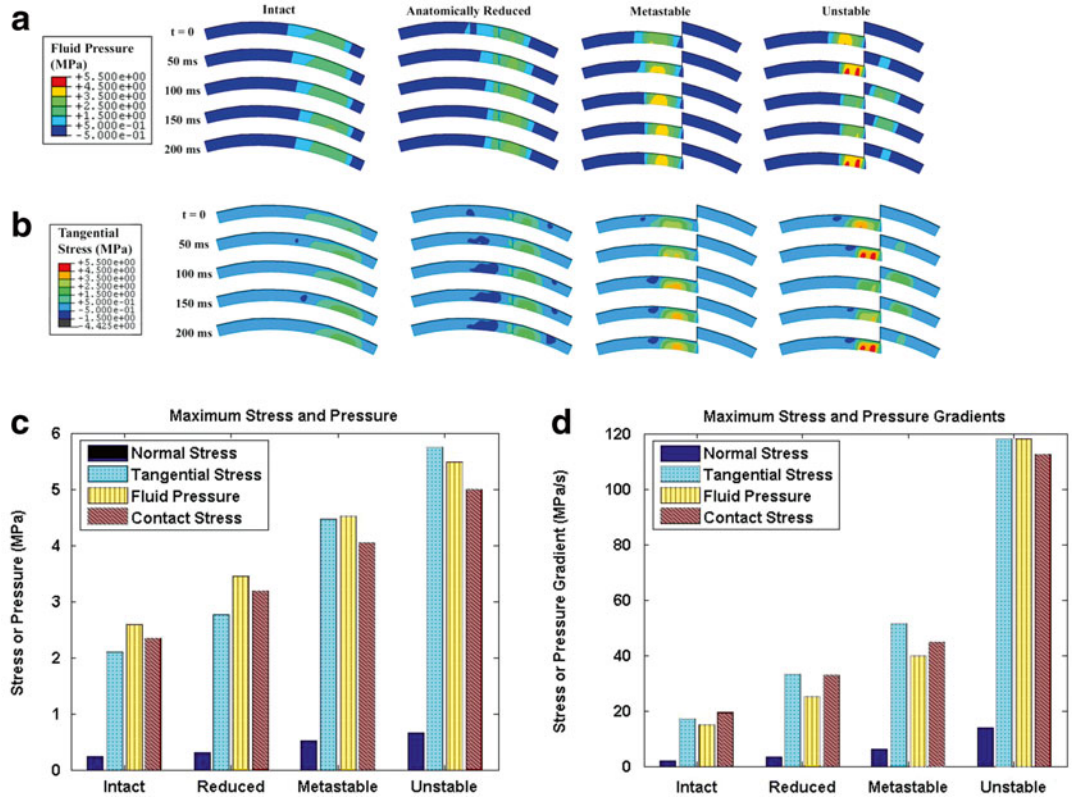

Fig. 9.3 Poroelastic two-dimensional finite element modeling of incongruous and unstable ankle motion demonstrated that both interstitial fluid pressure (**a**) and solid phase tangential stresses (**b**) significantly increased secondary to instability during the subluxation event ($t = 50$ ms) and when the talus reduced back under the distal tibia ($t = 200$ ms). Fluid pressure, normal stress, and shear (tangential) stress increased modestly in metastable and unstable specimens compared to intact and reduced specimens (**c**). In contrast, instability resulted in significant increases in temporal gradients of normal stress, shear stress, and fluid pressure compared to metastable, reduced, and intact conditions (**d**)

resulting from an incongruous articulation [28]. This was a two-dimensional model evaluating plane strain and two-dimensional stresses. Initially, the investigators validated the performance of the model by comparing results in congruous and stable ankles to finite element simulations. These comparisons included ankles that were entirely intact and in ankles that had an osteotomy that was anatomically reduced. Subsequently, they modeled a 2.0 mm coronal plane stepoff that simulated cadaveric ankle testing. Under these conditions, they simulated ankle flexion-extension in which the talus remained stable (metastable) under the tibia and conditions in which the talus subluxated anteriorly into the defect (unstable).

Interstitial fluid pressures and stresses increased in metastable and unstable conditions compared to reduced and intact conditions (Fig. 9.3a–c), but the increases were modest. In contrast, temporal gradients of fluid pressure, tangential (shear) stress, and normal stress all increased significantly in unstable conditions compared to metastable conditions. Solid-phase normal transient stress rates increased from approximately 4 MPa/s in metastable conditions to 14 MPa/s in unstable conditions (Fig. 9.3d). Likewise, temporal gradients of solid-phase tangential stresses and fluid pressures increased between 250 % and 300 % in unstable conditions compared to metastable conditions. Incongruity- and instability-related changes in stresses and stress rates were encountered throughout the entire thickness of the cartilage but were greater in the superficial and middle zones of cartilage.

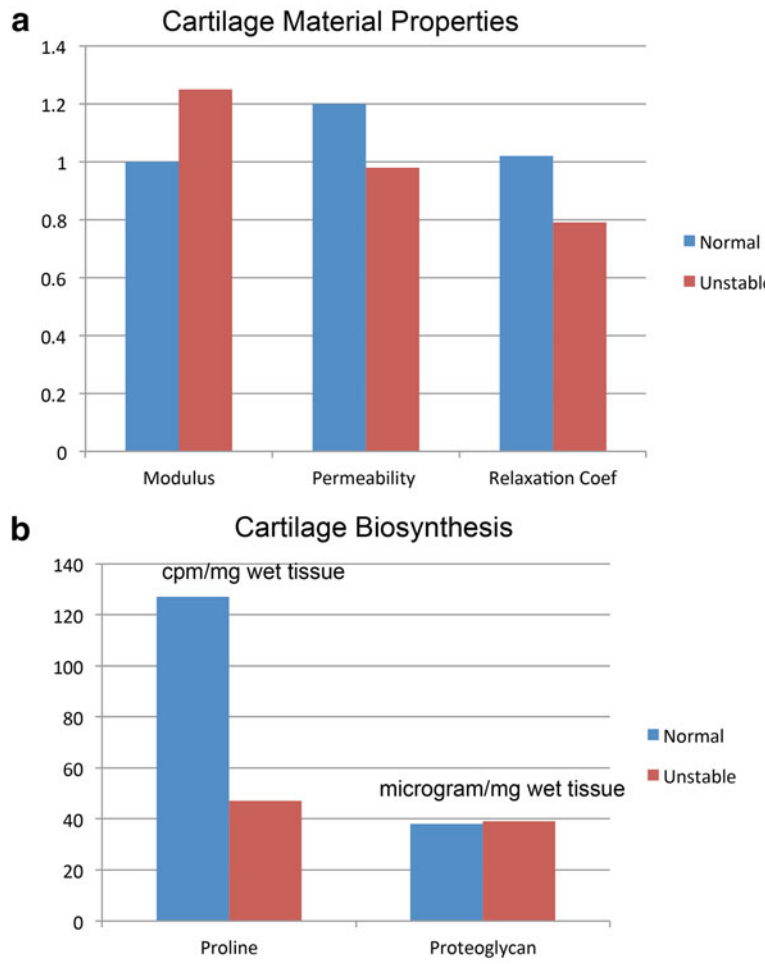

Fig. 9.4 Material property (**a**) and biochemical (**b**) changes in osteochondral specimens subjected to normal and unstable loads. Compared to preloading values, instability resulted in a modest rise in compressive modulus and decreases in permeability and relaxation coefficient compared to normally loaded specimens (**a**). These findings were corroborated in biochemical testing that demonstrated no changes in proteoglycan content but significant decreases in proline uptake consistent with disruption of the collagenous structure of cartilage in unstable specimens (**b**)

These findings demonstrated similar stress rate elevations compared to surface stress rates in cadaveric ankles. In addition, abnormal increases in interstitial stress rates dissipated throughout the thickness of the cartilage demonstrating how cartilage transduces abnormal surface loads to more uniform stresses in the deep layers of cartilage at the level of the subchondral plate.

Tissue-Level Models of Instability

Cartilage tissue is unique because it exists in vivo in relative anoxia and has no direct blood supply. This allows for explanted tissue-level investigations that can subject cartilage samples to prescribed mechanical perturbations and subsequently measure biosynthetic response under quasi-physiologic conditions.

In an ongoing series of experiments, investigators have subjected freshly explanted bovine tibial plateau osteochondral specimens to a series of repetitive loads. Explants were subjected to loading regimens representing normal loads (1.0 MPa applied at 10 MPa/s) and unstable loads (3 MPa applied at 100 MPa/s) [29]. Specimens were subjected to the prescribed loading regimen for 1,000 cycles at 1 Hz every other day for 2 weeks. In these specimens, materials testing demonstrated that unstable loads resulted in a 20 % increase in compressive modulus and a 20 % decrease in relaxation coefficient compared to normally loaded specimens (Fig. 9.4a). The investigators concluded that short-term exposure

to instability type stresses affected the collagenous matrix constituents of cartilage more so than the proteoglycan components. At the end of the testing period, cartilage biosynthesis as measured by proline uptake in specimens subjected to instability loading was 40 % of proline uptake in specimens subjected to normal loads (Fig. 9.4b). In contrast, proteoglycan content was unchanged between the two loading conditions.

In Vivo Models of Instability

In vitro cadaveric whole-joint mechanical tests yield information regarding changes articular surface stress transfer under pathologic conditions. However, these tests cannot determine tissue-level biologic response to changes in joint loading. Tissue-level testing in freshly harvested specimens has allowed investigators to determine how changes in loading parameters affect the biologic response of viable but isolated cartilage to various injurious loading regimens. However, these tests are reduced to evaluating isolated cartilage biologic responses to mechanical perturbations and cannot account for whole-joint biologic effects of injury. In vivo testing is necessary to truly investigate an organ-level response of a joint to injury or chronic changes in the prevailing loading environment. PTOA is an organ-level disease and ultimately the pathophysiology leading to PTOA needs to be described in survival organ-level investigations. Evidence continues to accumulate describing whole-joint responses to injury, highlighting contributions from cartilage and synovium to mechanical changes in loading.

There have been multiple models of ACL-transection instability used to study articular cartilage changes that result from ligament transaction [30]. Similar alterations of mechanical properties in articular cartilage that are observed in the human with osteoarthritis also occur in the canine after 12 weeks ACL transection [31]. However, rigorous measuring of post-transection instability was not done as a part of this type of investigation. Recently, an in vivo model of joint instability, in which instability was quantified, was developed to investigate the effect of increasing instability on cartilage degeneration and biologic response [32]. In this test, the investigators developed a model of graded instability in rabbit knees to determine the mechanical and biologic effect of instability on an intact joint. Rabbits were subjected to an anterior parapatellar arthrotomy, allowing the anterior cruciate ligament (ACL) to be isolated. Subsequently, graded portions of the ACL were transected. Immediately after transection, the anesthetized rabbits were subjected to sagittal plane translational stability testing using purpose-designed fixturing to quantify the instability resulting from ligament transection. Both the tibia and femur were secured with Steinmann pins which articulated with a custom mechanical actuator that applied a linear displacement to the tibia while the femur was statically stationed. Force/displacement curves were plotted to determine knee stiffness, allowing the investigators to quantify translational kinematics in transaction specimens compared to normal controls. The stiffness of the linear portion of the force displacement curve was a designated surrogate for instability. The laxity encompassing the neutral zone (the "toe" region in the force displacement curve representing normal laxity surrounding the resting position of the ligament around zero displacement) was also quantified. Both the linear stiffness and neutral zone laxity were found to be directly related to the percentage of ACL transaction.

Two experimental groups of rabbits were compared to sham-operated control specimens [33]. Experimental groups had either a complete or partial transaction of their ACL. Partial transection specimens had approximately 50 % of their ACL transected. Sham controls had an arthrotomy but no ligament transection. Complete transection of the ACL decreased translational stiffness by 70 % and doubled the neutral zone laxity compared to sham controls (Fig. 9.5a). Partial transection did not affect neutral zone laxity and decreased translational stiffness 30 % compared to sham controls (Fig. 9.5a). Eight weeks after surgery, Mankin cartilage scores correlated closely with post-transection stiffness demonstrating a linear relationship between joint

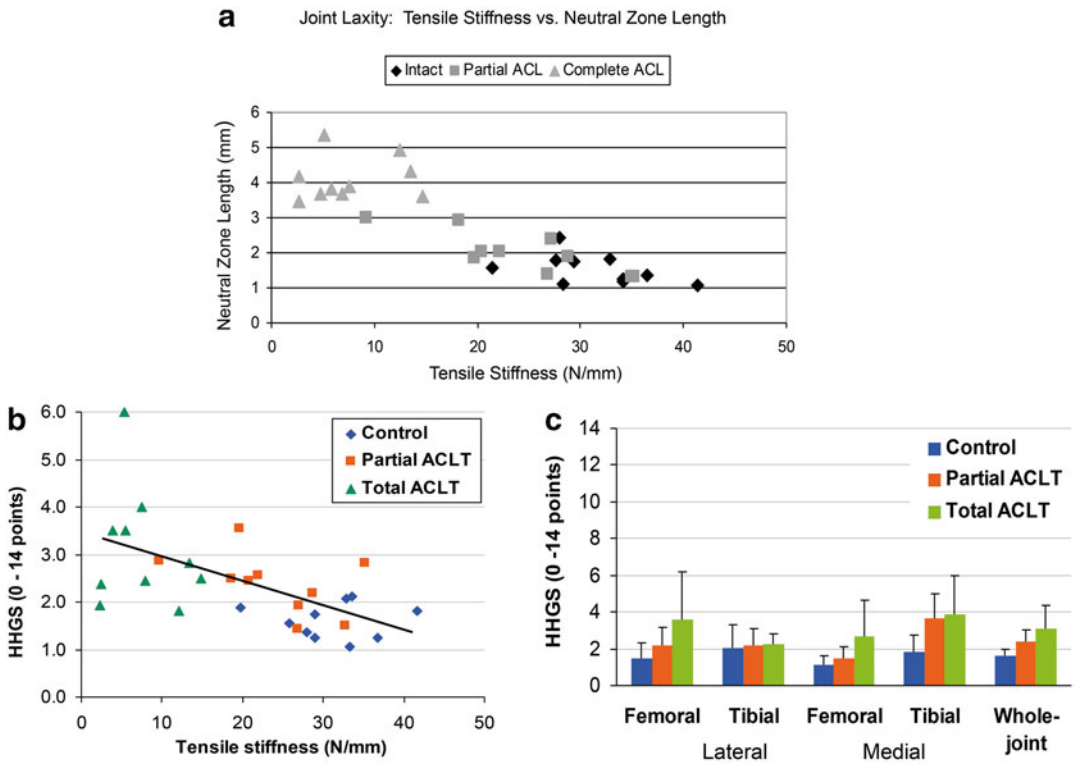

Fig. 9.5 Graded instability created in rabbit knees by progressive ACL sectioning decreased stiffness in both partial and completely transected specimens and increased neutral zone laxity in complete transaction specimens (**a**). PTOA correlated closely with resulting decreases in stiffness (**b**). Degenerative changes correlated were increased in partial and complete transaction specimens with significant differences measured between partial and complete transaction specimens (**c**)

stiffness and whole-joint degenerative changes (Fig. 9.5b). The greatest degenerative changes were encountered in the medial tibial plateau surface (Fig. 9.5c). This experiment clearly demonstrated that in vivo instability is directly related to cartilage degeneration.

A subsequent in vivo model of rabbit knee instability was developed to reduce the magnitude of experimentally induced trauma to the rabbit knee [34]. In this model a minimally invasive posterior arthrotomy was performed with rabbits positioned prone accessing the posterior knee joint. This allowed access to the posterior weight-bearing surface of the medial femoral condyle (the majority of load transfer in the rabbit knee occurs through the posterior part of the femoral condyle) and the posterior attachment of the medial meniscus. In this model, transection of the posterior horn of the medial meniscus resulted in nearly identical changes in medial knee load transfer compared to total medial meniscectomy (Fig. 9.6a, b). Animals were sacrificed at either 8 or 26 weeks after surgery. At 8 weeks, degenerative changes had occurred primarily in the medial tibial plateau (Fig. 9.6c). However, at 26 weeks, significant degeneration had progressed in the medial knee with increasing Mankin scores in both the medial tibial plateau and medial femoral condyle (Fig. 9.6c).

In a follow-up study, the investigators hypothesized that impact injury would potentiate instability-associated progression of articular surface degeneration [35]. In this study, the medial femoral condyle was impacted through the posterior arthrotomy at three different energy levels. The posterior horn medial meniscus destabilization technique was then applied to a group of experimental animals from each impact level.

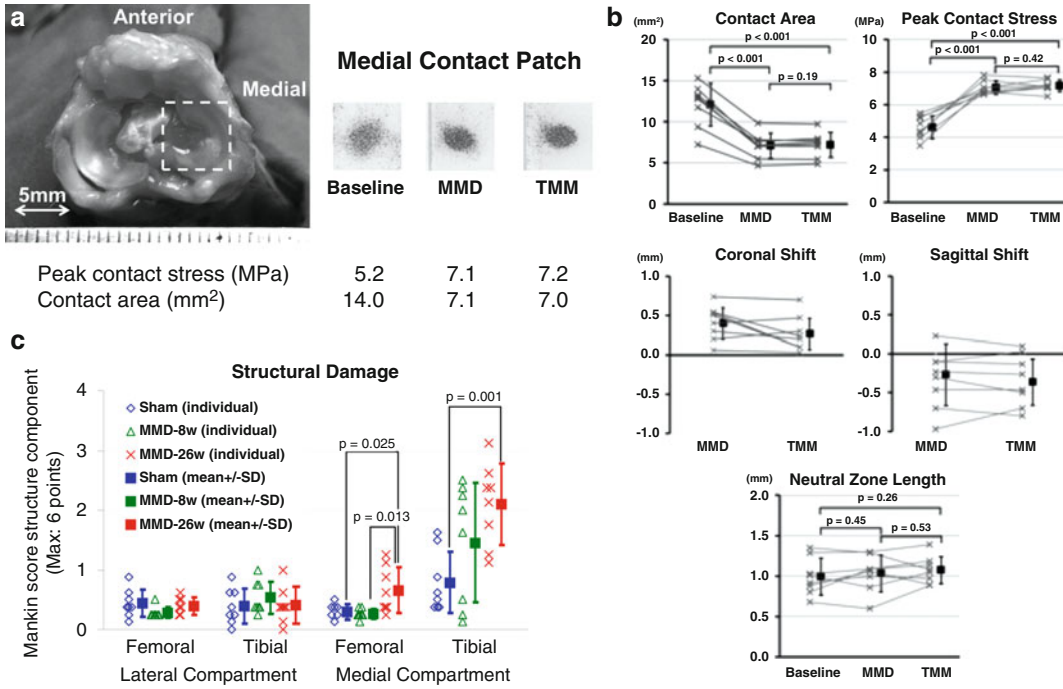

Fig. 9.6 A new in vivo model of instability can produce significant changes in loading area and peak stress with minimal joint invasion by releasing the posterior horn of the medial meniscus in the rabbit knee (**a**, **b**). This results in progressive degeneration, particularly concentrated in the medial knee compartment (**c**)

Histologic data confirmed that destabilizing the meniscus significantly exacerbated impact-related articular surface degeneration 8 weeks after injury. In addition, the degenerative changes progressed between 8 weeks and 26 weeks after injury.

Recently, gait analyses have been performed on both a rat model and sheep model of knee instability. Rats were subjected to division of their medial collateral ligament in concert with transaction of their medial meniscus. Gait analysis demonstrated significant shift of weight away from the affected limb which was progressive from days 9 to 24 after surgery. Follow-up analyses showed that joint degeneration and inflammatory cytokines were elevated in experimental joints [36]. Sheep knees were subjected to combination ACL/MCL transections. Twenty weeks after surgery, significant gait and knee kinematic abnormalities correlated closely with joint degeneration [37].

In summary, in vivo models of whole-joint degeneration resulting from instability have been created using small animal and large animal models. Preliminary data from these models have shown that instability reliably produces articular surface degeneration. The details of mechanotransduction of the abnormal joint mechanics secondary to instability into a physiologic and cellular response leading to PTA are unknown. In addition, therapies to mitigate hazardous mechanotransduction or improve the mechanics are untested. These models represent viable investigative tools to describe pathophysiologic cascades that link instability to PTOA and to survey treatments to mitigate PTOA in unstable joints.

Conclusions

Injuries resulting in chronically unstable joints predictably progress to PTOA, especially in the major weight-bearing joints. Therefore, it is important to understand the mechanical and biological effects of instability and to understand how instability results in pathologic mechanotransduction of unstable surface stresses into

degenerative biologic responses. Fortunately, recent improvements in analytical techniques have created new testing capabilities allowing investigators to model and investigate instability in a variety of settings. Accurate and validated real-time stress transducers have facilitated tests that have quantified relevant loads resulting from physiologically relevant whole-joint instability tests. These findings have highlighted the hazardous stress rates that occur during subluxation. Tissue explant experimentation has opened doors to quantify tissue-level biologic responses to a variety of loading environments including unstable loads. These experiments allow precise measurements of cartilage biologic response under unstable conditions but cannot account for living whole-joint responses to injury. Finally, investigators have developed techniques to quantify instability in survival models facilitating experiments that can account for living joint level biologic responses to unstable joints. Survival experiments have consistently de*m*onstrated instability-associated joint deterioration. These models will allow therapeutic interventions to be investigated.

References

1. Korkmaz A, Ciftdemir M, Ozcan M, Copuroglu C, Saridogan K. The analysis of the variables, affecting outcome in surgically treated tibia pilon fractured patients. Injury. 2013;44(10):1270–4.
2. Matta JM. Fractures of the acetabulum: accuracy of reduction and clinical results in patients managed operatively within three weeks after the injury. J Bone Joint Surg Am. 1996;78(11):1632–45.
3. Matta JM. Operative treatment of acetabular fractures through the ilioinguinal approach: a 10-year perspective. J Orthop Trauma. 2006;20(1 Suppl):S20–9.
4. Tannast M, Najibi S, Matta JM. Two to twenty-year survivorship of the hip in 810 patients with operatively treated acetabular fractures. J Bone Joint Surg Am. 2012;94(17):1559–67.
5. Fitzpatrick DC, Foels WS, Pedersen DR, Marsh JL, Saltzman CL, Brown TD. An articulated ankle external fixation system that can be aligned with the ankle axis. Iowa Orthop J. 1995;15:197–203.
6. Lansinger O, Bergman B, Korner L, Andersson GB. Tibial condylar fractures. A twenty-year follow-up. J Bone Joint Surg Am. 1986;68(1):13–9.
7. Marsh JL, Bonar S, Nepola JV, Decoster TA, Hurwitz SR. Use of an articulated external fixator for fractures of the tibial plafond. J Bone Joint Surg Am. 1995; 77(10):1498–509.
8. Stevens DG, Beharry R, McKee MD, Waddell JP, Schemitsch EH. The long-term functional outcome of operatively treated tibial plateau fractures. J Orthop Trauma. 2001;15(5):312–20.
9. Delamarter RB, Hohl M, Hopp Jr E. Ligament injuries associated with tibial plateau fractures. Clin Orthop. 1990;250:226–33.
10. Hall JA, Beuerlein MJ, McKee MD, Canadian Orthopaedic Trauma Society. Open reduction and internal fixation compared with circular fixator application for bicondylar tibial plateau fractures. Surgical technique. J Bone Joint Surg Am. 2009; 91 Suppl 2 Pt 1:74–88.
11. Honkonen SE. Indications for surgical treatment of tibial condyle fractures. Clin Orthop. 1994;302: 199–205.
12. Lubbeke A, Salvo D, Stern R, Hoffmeyer P, Holzer N, Assal M. Risk factors for post-traumatic osteoarthritis of the ankle: an eighteen year follow-up study. Int Orthop. 2012;36(7):1403–10.
13. Volpin G, Dowd GS, Stein H, Bentley G. Degenerative arthritis after intra-articular fractures of the knee. Long-term results. J Bone Joint Surg Br. 1990;72(4):634–8.
14. Marti RK, Raaymakers EL, Nolte PA. Malunited ankle fractures. The late results of reconstruction. J Bone Joint Surg Br. 1990;72(4):709–13.
15. Brown TD, Anderson DD, Nepola JV, Singerman RJ, Pedersen DR, Brand RA. Contact stress aberrations following imprecise reduction of simple tibial plateau fractures. J Orthop Res. 1988;6(6):851–62.
16. Lefkoe TP, Walsh WR, Anastasatos J, Ehrlich MG, Barrach HJ. Remodeling of articular step-offs. Is osteoarthrosis dependent on defect size? Clin Orthop. 1995;314:253–65.
17. Nelson BH, Anderson DD, Brand RA, Brown TD. Effect of osteochondral defects on articular cartilage. Contact pressures studied in dog knees. Acta Orthop Scand. 1988;59(5):574–9.
18. Mow VC, Kuei SC, Lai WM, Armstrong CG. Biphasic creep and stress relaxation of articular cartilage in compression? Theory and experiments. J Biomech Eng. 1980;102(1):73–84.
19. Guilak F, Ratcliffe A, Lane N, Rosenwasser MP, Mow VC. Mechanical and biochemical changes in the superficial zone of articular cartilage in canine experimental osteoarthritis. J Orthop Res. 1994;12(4):474–84.
20. Oloyede A, Flachsmann R, Broom ND. The dramatic influence of loading velocity on the compressive response of articular cartilage. Connect Tissue Res. 1992;27(4):211–24.
21. Lee DA, Bader DL. Compressive strains at physiological frequencies influence the metabolism of chondrocytes seeded in agarose. J Orthop Res. 1997; 15(2):181–8.
22. Sah RL, Kim YJ, Doong JY, Grodzinsky AJ, Plaas AH, Sandy JD. Biosynthetic response of cartilage explants to dynamic compression. J Orthop Res. 1989;7(5):619–36.
23. Atkinson TS, Haut RC, Altiero NJ. Impact-induced fissuring of articular cartilage: an investigation of failure criteria. J Biomech Eng. 1998;120(2):181–7.

24. Kurz B, Jin M, Patwari P, Cheng DM, Lark MW, Grodzinsky AJ. Biosynthetic response and mechanical properties of articular cartilage after injurious compression. J Orthop Res. 2001;19(6):1140–6.
25. Lewis JL, Deloria LB, Oyen-Tiesma M, Thompson Jr RC, Ericson M, Oegema Jr TR. Cell death after cartilage impact occurs around matrix cracks. J Orthop Res. 2003;21(5):881–7.
26. McKinley TO, Tochigi Y, Rudert MJ, Brown TD. Instability-associated changes in contact stress and contact stress rates near a step-off incongruity. J Bone Joint Surg Am. 2008;90(2):375–83.
27. McKinley TO, Tochigi Y, Rudert MJ, Brown TD. The effect of incongruity and instability on contact stress directional gradients in human cadaveric ankles. Osteoarthritis Cartilage. 2008;16(11):1363–9.
28. Goreham-Voss CM, McKinley TO, Brown TD. A finite element exploration of cartilage stress near an articular incongruity during unstable motion. J Biomech. 2007;40(15):3438–47.
29. Heiner AD, McKinley TO, Ramakrishnan PS, Bierman JF, Martin JA. Normal versus abnormal loading of cartilage explants. San Antonio, TX: Orthopaedic Research Society; 2013.
30. Dedrick DK, Goldstein SA, Brandt KD, O'Connor BL, Goulet RW, Albrecht M. A longitudinal study of subchondral plate and trabecular bone in cruciate-deficient dogs with osteoarthritis followed up for 54 months. Arthritis Rheum. 1993;36(10):1460–7.
31. Setton LA, Elliott DM, Mow VC. Altered mechanics of cartilage with osteoarthritis: human osteoarthritis and an experimental model of joint degeneration. Osteoarthritis Cartilage. 1999;7(1):2–14.
32. Heiner AD, Rudert MJ, McKinley TO, Fredericks DC, Bobst JA, Tochigi Y. In vivo measurement of translational stiffness of rabbit knees. J Biomech. 2007;40(10):2313–7.
33. Tochigi Y, Vaseenon T, Heiner AD, Fredericks DC, Martin JA, Rudert MJ, Hillis SL, Brown TD, McKinley TO. Instability dependency of osteoarthritis development in a rabbit model of graded anterior cruciate ligament transection. J Bone Joint Surg Am. 2011;93(7):640–7.
34. Vaseenon T, Tochigi Y, Heiner AD, Goetz JE, Baer TE, Fredericks DC, Martin JA, Rudert MJ, Hillis SL, Brown TD, et al. Organ-level histological and biomechanical responses from localized osteoarticular injury in the rabbit knee. J Orthop Res. 2011;29(3):340–6.
35. Arunakul M, Tochigi Y, Goetz JE, Diestelmeier BW, Heiner AD, Rudert J, Fredericks DC, Brown TD, McKinley TO. Replication of chronic abnormal cartilage loading by medial meniscus destabilization for modeling osteoarthritis in the rabbit knee in vivo. J Orthop Res. 2013;31(10):1555–60.
36. Allen KD, Mata BA, Gabr MA, Huebner JL, Adams Jr SB, Kraus VB, Schmitt DO, Setton LA. Kinematic and dynamic gait compensations resulting from knee instability in a rat model of osteoarthritis. Arthritis Res Ther. 2012;14(2):R78.
37. Frank CB, Beveridge JE, Huebner KD, Heard BJ, Tapper JE, O'Brien EJ, Shrive NG. Complete ACL/MCL deficiency induces variable degrees of instability in sheep with specific kinematic abnormalities correlating with degrees of early osteoarthritis. J Orthop Res. 2012;30(3):384–92.